FDG-PET hypometabolism is more sensitive than MRI atrophy in Parkinson's disease: A whole-brain multimodal imaging meta-analysis

Franziska Albrecht[a,*,1], Tommaso Ballarini[a,1], Jane Neumann[a,c,d], Matthias L. Schroeter[a,b]

[a] Max Planck Institute for Human Cognitive and Brain Sciences, Leipzig, Germany
[b] Clinic of Cognitive Neurology, University of Leipzig & FTLD Consortium Germany, Leipzig, Germany
[c] Leipzig University Medical Center, IFB Adiposity Diseases, Leipzig, Germany
[d] Department of Medical Engineering and Biotechnology, University of Applied Science, Jena, Germany

ARTICLE INFO

ABSTRACT

Recently, revised diagnostic criteria for Parkinson's disease (PD) were introduced (Postuma et al., 2015). Yet, except for well-established dopaminergic imaging, validated imaging biomarkers for PD are still missing, though they could improve diagnostic accuracy.

We conducted systematic meta-analyses to identify PD-specific markers in whole-brain structural magnetic resonance imaging (MRI), [18F]-fluorodeoxyglucose-positron emission tomography (FDG-PET) and diffusion tensor imaging (DTI) studies. Overall, 74 studies were identified including 2323 patients and 1767 healthy controls. Studies were first grouped according to imaging modalities (MRI 50; PET 14; DTI 10) and then into subcohorts based on clinical phenotypes. To ensure reliable results, we combined established meta-analytical algorithms - anatomical likelihood estimation and seed-based D mapping - and cross-validated them in a conjunction analysis.

Glucose hypometabolism was found using FDG-PET extensively in bilateral inferior parietal cortex and left caudate nucleus with both meta-analytic methods. This hypometabolism pattern was confirmed in subcohort analyses and related to cognitive deficits (inferior parietal cortex) and motor symptoms (caudate nucleus). Structural MRI showed only small focal gray matter atrophy in the middle occipital gyrus that was not confirmed in subcohort analyses. DTI revealed fractional anisotropy reductions in the cingulate bundle near the orbital and anterior cingulate gyri in PD.

Our results suggest that FDG-PET reliably identifies consistent functional brain abnormalities in PD, whereas structural MRI and DTI show only focal alterations and rather inconsistent results. In conclusion, FDG-PET hypometabolism outperforms structural MRI in PD, although both imaging methods do not offer disease-specific imaging biomarkers for PD.

1. Introduction

Among neurodegenerative diseases, Parkinson's disease (PD) is the second most common disorder with annually 5–35 new cases per 100,000 persons (Poewe et al., 2017). In the last two decades, research on PD has shed new light on its clinical characterization and pathogenesis. However, the most often used diagnostic criteria were published back in 1992 by the Parkinson's Disease Society Brain Bank (PDSBB) (Hughes et al., 1992). These are based on the clinical observation of the parkinsonian syndrome, defined as bradykinesia plus one of rigidity, tremor at rest or postural instability, combined with

fulfilling both exclusion and supportive positive prospective criteria, such as levodopa responsiveness and asymmetry of the motor impairment (Hughes et al., 1992). Beyond motor-symptoms, PD may show also non-motor manifestations, such as sleep disorder, anosmia, constipation, hallucinations, and cognitive impairment possibly leading to dementia (Poewe et al., 2017; Schapira et al., 2017). This is shifting the conceptualization of PD from a pure dopaminergic motor syndrome to a multisystem and multi-neurotransmitter one (Titova et al., 2017). The recently updated PD diagnostic criteria by the Movement Disorder Society have already included the current clinical knowledge of PD research, comprising non-motor features, thus increasing diagnostic

* Corresponding author at: Max Planck Institute for Human Cognitive and Brain Sciences, Stephanstr. 1A, 04103 Leipzig, Germany.
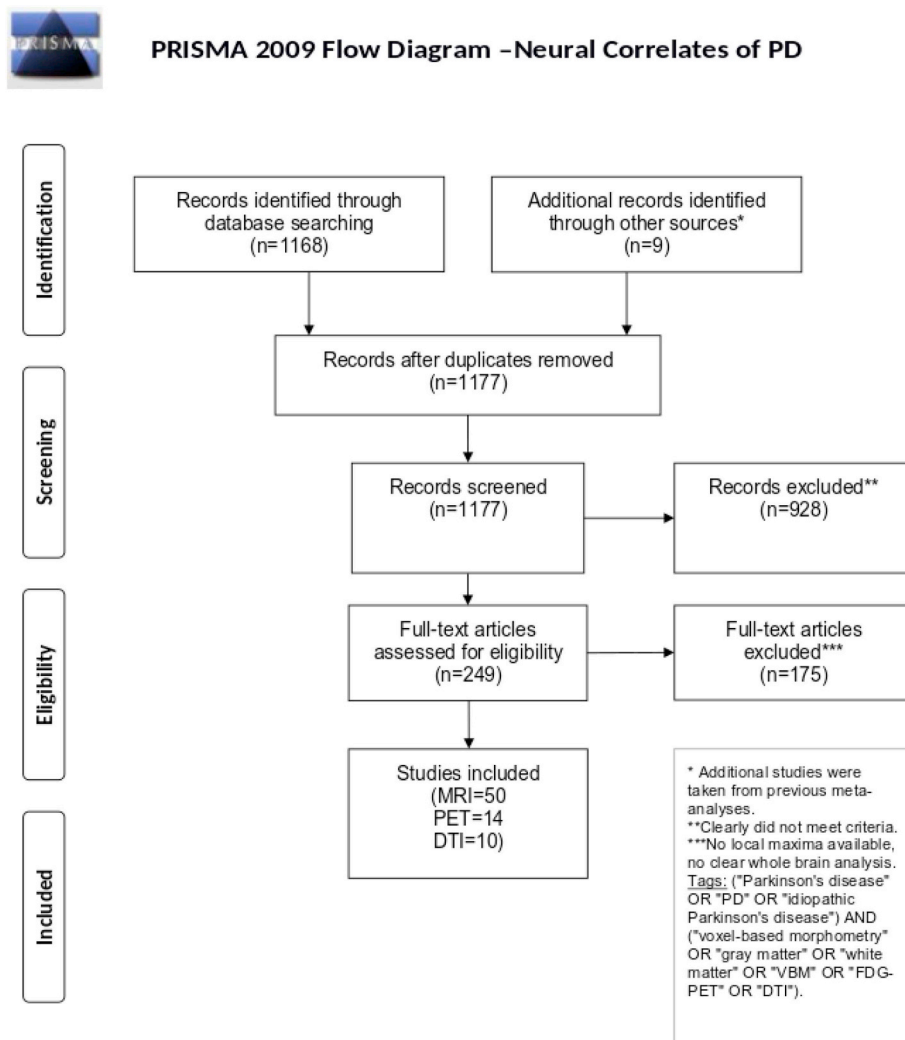E-mail addresses: falbrecht@cbs.mpg.de (F. Albrecht), tommaso@cbs.mpg.de (T. Ballarini), neumann@cbs.mpg.de (J. Neumann), schroet@cbs.mpg.de (M.L. Schroeter).
[1] Joined first authorship.

Please cite this article as: Albrecht, F., NeuroImage: Clinical, https://doi.org/10.1016/j.nicl.2018.11.004

Fig. 1. PRISMA statement flow diagram. Flow of information through different phases of the systematic literature search identifying the neural correlates of Parkinson's disease. Image modified according to the PRISMA statement (Moher et al., 2009).

accuracy (Postuma et al., 2015). Nevertheless, the diagnosis is still predominantly based on clinical symptoms. Indeed, the only brain biomarker mentioned, i.e. normal presynaptic dopaminergic function as detected by molecular imaging, is used as an exclusion criterion for PD (Postuma et al., 2015). A recent meta-analysis has already provided a synthesis of studies investigating presynaptic dopamine function in PD (Kaasinen and Vahlberg, 2017). No other imaging biomarkers have been included so far for the diagnosis of PD, although they could be crucial to improve the diagnostic accuracy. In this respect, Alzheimer's disease research is exemplary. Indeed, magnetic resonance imaging (MRI) and amyloid and [18F]-fluorodeoxyglucose (FDG) positron emission tomography (PET) have been successfully integrated in the most recent diagnostic criteria for mild cognitive impairment, as a pre-stage, and Alzheimer's disease (Albert et al., 2011; Dubois et al., 2014). Along the same line, disease-specific imaging biomarkers have been also proposed for other neurodegenerative diseases, such as fronto-temporal lobar degeneration or primary progressive aphasia (Gorno-Tempini et al., 2011; Rascovsky et al., 2011). The identification of PD-specific imaging biomarkers based on MRI or FDG-PET imaging could provide a useful tool to improve the differential diagnosis, for example in comparison to atypical parkinsonism.

Up to date, many studies have tried to identify new imaging biomarkers for PD (Lehericy et al., 2017; Lotankar et al., 2017; Postuma and Berg, 2016). Recent qualitative reviews about multimodal biomarkers in PD suggested diffusion tensor imaging (DTI) as preferably useful for diagnosis and staging of PD (Lehericy et al., 2017; Tuite, 2017). Indeed, a pattern recognition algorithm (support vector machine classification) using DTI data of the substantia nigra has proved to yield high accuracy (up to 97.5%) in differentiating PD from healthy subjects and other parkinsonian syndromes (Haller et al., 2012). Also other MRI- and FDG-PET-based measures have been investigated by many studies. However, due to the large variability between study settings and analysis methods, the reported results are heterogeneous and consequently they are considered as still developing methods for PD assessment (Lehericy et al., 2017; Lotankar et al., 2017; Postuma and Berg, 2016). In order to provide an unbiased overview of the up-to-date literature,

free from a priori hypotheses, we decided to focus our meta-analysis on whole-brain studies applying structural MRI, FDG-PET or DTI imaging. For a complete account of the literature, the reader can refer to the references in the Supplementary material. To further disentangle the effects of different clinical phenotypes, we stratified our findings into several clinical subcohorts. Our aim was to identify a robust and replicable neural signature of PD that can be used in the research and clinical settings. To this end, we systematically applied quantitative data-driven meta-analyses on multimodal neuroimaging data to identify prototypical neural networks involved in PD and to extract disease-specific imaging biomarkers. Moreover, we aimed to compare the different imaging modalities by directly contrasting them. However, given the limited number of DTI studies performing whole-brain analysis, this comparison could be performed only between MRI and FDG-PET. Of note, to cross-validate our results, we used a unique approach integrating two meta-analytical algorithms.

2. Materials and methods

2.1. Study selection

Literature search and study selection were performed according to the Preferred Reporting Items for Systematic reviews and Meta-Analyses (PRISMA) statement (www.prisma-statement.org), to assure high quality and reproducibility. First, we searched PubMed for studies published until November 2016 and matching the following keywords: ("Parkinson's disease" OR "PD" OR "idiopathic Parkinson's disease") AND ("voxel-based morphometry" OR "gray matter" OR "white matter" OR "VBM" OR "FDG-PET" OR "DTI"). Only studies satisfying the following criteria were further considered: (1) original and peer-reviewed study, (2) established diagnostic criteria for PD diagnosis[2], (3) whole-brain neuroimaging analysis, (4) comparison with age-matched healthy controls, and (5) result coordinates reported in stereotactic reference systems, e.g. Talairach or Montreal Neurological Institute (MNI). To prevent any a priori assumptions, region-of-interest analyses and case studies were excluded. The selection is summarized in the PRISMA flowchart (Fig. 1). Both literature search and study selection were independently performed by two investigators (FA and TB).

FDG-PET and structural voxel-based morphometry MRI (MRI-VBM) studies were numerous enough to be stratified into subcohorts. Specifically, three subcohorts were created according to the PD patients' clinical characteristics: (1) an inclusive group comprising all PD patients irrespective of their clinical features (e.g. cognitive impairment or visual hallucinations) (PD-All), (2) a subgroup including only PD patients with cognitive impairment, defined as Mild Cognitive Impairment or dementia (PD-Cog), (3) a subgroup of patients with only PD motor symptoms without specific cognitive or behavioral deficits (PD-Motor). Additional subanalyses were run on structural MRI studies reporting gray matter increases in PD as compared to controls (PD-Inc) and white matter changes in PD (PD-WM). Furthermore, white matter changes were also investigated in DTI fractional anisotropy studies.

2.2. Statistical analyses

2.2.1. Demographic and clinical features

The following variables were extracted across studies: age, gender, Mini-Mental State Examination (MMSE), disease duration, Hoehn&Yahr stage, and Unified Parkinson's Disease Rating Scale motor score (UPDRS–III). Summary statistics (i.e. means and standard deviations) were computed across all the studies (MRI + PET + DTI), as well as separately for the clinical subgroups (i.e. PD-All, PD-Motor, PD-Cog, and PD-Inc) and imaging modalities (Table 1). Group comparisons by means of Kruskal-Wallis tests were conducted to statistically assess differences in the extracted variables across different imaging cohorts. Multiple statistical tests were Bonferroni corrected with $\alpha = 0.01$.

2.2.2. Meta-analysis

Statistical analyses were performed with two different software packages to obtain robust, reliable results and to validate the results of each individual technique. Anatomical Likelihood Estimation (ALE) and Seed-based *D* Mapping (SDM) approaches are implemented in Ginger ALE (v2.3.6) (Eickhoff et al., 2012) and SDM (v5.141) (Radua and Mataix-Cols, 2009) (Table-e11 summarizes characteristics of both methods).

First, we applied the SDM approach (Radua and Mataix-Cols, 2012; Radua et al., 2014). In brief, the extracted maxima from the literature are used to build a statistical map for each study. A value is assigned to each voxel in the map depending on its proximity to the reported coordinates of interest, so that the closer the voxel, the higher its value. In the case of voxels that lie in the proximity of more than one coordinate, the values are linearly summed. To avoid the issue of studies reporting coordinates in close proximity, a multilevel kernel density analysis is implemented to limit the values to a maximum. Then, pooling the individual maps together, a mean meta-analytical map is computed, in which the value of a voxel is defined as the proportion of studies reporting a coordinate around that voxel. Finally, the resulting map is tested against a whole-brain null distribution of the meta-analytical values (Radua and Mataix-Cols, 2009). Of note, the SDM software does not provide a built-in function for multiple comparison correction. Accordingly, we performed false discovery rate (FDR) correction of the uncorrected *p*-values using the SDM FDR online calculator.

For SDM analyses, the extracted coordinates of gray matter density, metabolic or fractional anisotropy changes and the corresponding z-scores were used. In case of reported *t*-values, a t-to-z conversion was performed (www.sdmproject.com/utilities/?show=Statistics). Coordinates were converted into MNI space by the software. The null distribution was computed with 100 randomizations and an anisotropic kernel. The first threshold was set at $p < .001$ uncorrected. In addition, to test the stability of the results, a jack-knife approach was applied, i.e. removing one study at a time and running the analysis again. We thus report only clusters present in at least 80% of the jack-knife folds for the PD-All analysis and the full range (1–100%) for the subanalyses on limited number of studies. Notably, the SDM software takes into account the sample size differences between the included studies and it allows also the inclusion of studies with negative findings.

Secondly, the same meta-analysis was run by means of the ALE method (Eickhoff et al., 2012; Laird et al., 2009). In summary, each coordinate is set as the center of a Gaussian probability distribution, whose width is corrected according to the sample size of the corresponding study. Then, all the Gaussian distributions are summed in one statistical map that is tested voxel-wise against the null hypothesis of an equal spatial distribution of the foci. Thus, regions with ALE values higher than expected by chance are identified.

We converted Talairach coordinates into MNI space with Lancaster transformation as implemented in GingerALE. The statistical threshold at the voxel-level was set at $p < .001$ uncorrected as in SDM. Results were considered significant after Family-Wise Error (FWE) correction at the cluster level ($p < .05$). In contrast to SDM, studies reporting negative findings cannot be included in the ALE meta-analysis and were thus discarded. Furthermore, to enable direct comparison of FDG-PET and MRI-VBM results, we run a contrast analysis between the two modalities on the PD-all cohort. This analysis, which statistically assesses differences between two modalities, is only implemented in GingerALE and was performed with standard parameters, i.e. uncorrected voxel-level threshold at $p < .001$ and 10,000 permutations.

Finally, to facilitate the comparison of results of both meta-analytic approaches, we created an overlap image combining them (SDM∩ALE). This conjunction analysis revealed clusters that were significant by both algorithms. In the following results and discussion sections we focus on brain changes in PD that were consistently identified by SDM and ALE meta-analyses. This highlights the most reliable findings that are independent from the specifics of the applied meta-analytical method.

F. Albrecht et al.

Table 1
Summarized subjects' demographics.

Cohort	Modality	Cohorts	Patients	Age (years)	Disease duration (years)	MMSE	UPDRS-III	Hoehn and Yahr
		N total (N in studies with null-findings, %)	N total (N in studies with null-findings, %)					
PD-All	FDG-PET	19 (3, 15.8%)	295 (46, 15.6%)	65.9 ± 4.9	8.4 ± 4.6	26.1 ± 5.0	29.8 ± 20.5	2.7 ± 0.9
	MRI	65 (18, 27.7%)	1767 (475, 26.9%)	66.0 ± 5.8	7.1 ± 4.5	25.2 ± 7.9	18.6 ± 10.9	1.5 ± 1.0
	DTI	11 (3, 27.3%)	212 (74, 34.9%)	62.5 ± 4.6	5.4 ± 2.6	28.1 ± 1.7	32.5 ± 17.0	1.8 ± 0
	Combined	95 (21, 22.1%)	2274 (595, 26.2%)	65.6 ± 5.5	7.2 ± 4.4	25.7 ± 7.0	22.4 ± 14.9	1.9 ± 1.1
PD-Motor	FDG-PET	13 (3, 23.1%)	240 (46, 19.2%)	64.8 ± 4.6	7.3 ± 4.2	26.1 ± 5.2	30.1 ± 23.0	2.5 ± 0.9
	MRI*	42 (13, 31.0%)	1177 (368, 31.3%)	64.5 ± 5.5	6.8 ± 2.8	27.8 ± 1.2	24.0 ± 7.2	2.1 ± 0.4
	Combined	55 (16, 29.1%)	1417 (414, 29.2%)	64.6 ± 5.2	7.0 ± 3.3	27.3 ± 3.2	25.7 ± 13.6	2.2 ± 0.6
PD-Cog	FDG-PET	5 (0, 0%)	92 (0, 0.0%)	69.0 ± 5.1	10.7 ± 5.7	20.7 ± 7.4	20.9 ± 8.8	3.3 ± 0.4
	MRI	11 (1, 9.1%)	256 (36, 14.1%)	71.1 ± 3.1	7.6 ± 3.9	24.0 ± 4.3	29.7 ± 7.3	2.7 ± 0.8
	Combined	15 (1, 6.7%)	348 (36, 10.3%)	70.4 ± 3.8	8.7 ± 4.7	23.4 ± 4.7	27.3 ± 8.3	2.9 ± 0.8
PD-WM	MRI	4/6 (2, 33.3%)	139 (64, 46.0%)	63.8 ± 2.5	7.0 ± 3.0	28.5 ± 0.8	22.6 ± 6.4	2.2 ± 0.7
PD-Inc	MRI	5 (0, 0%)	57 (0, 0.0%)	59.5 ± 7.5	8.1 ± 4.6	26.0 ± NA[(1)]	22.2 ± 0.8	2.1 ± 0.1

Note: Data shown as mean ± standard deviation. Cohorts reporting null findings were subsequently excluded in our meta-analysis. *The MRI meta-analyses led to non-significant results for the PD-Motor cohort, hence we do not elaborate on the results. [(1)]Only one study reported a value.
Abbreviations: DTI diffusion tensor imaging, MMSE Mini-Mental State Examination, MRI magnetic resonance imaging, NA not reported, PD-All all Parkinson's disease patients, PD-Cog Parkinson's disease patients with cognitive impairment, PD-Motor Parkinson's disease patients with motor impairment, PD-WM white matter atrophy in Parkinson's disease, FDG-PET [18F]-fluorodeoxyglucose-positron emission tomography, UPDRS-III motor score of Unified Parkinson Disease Rating Scale.
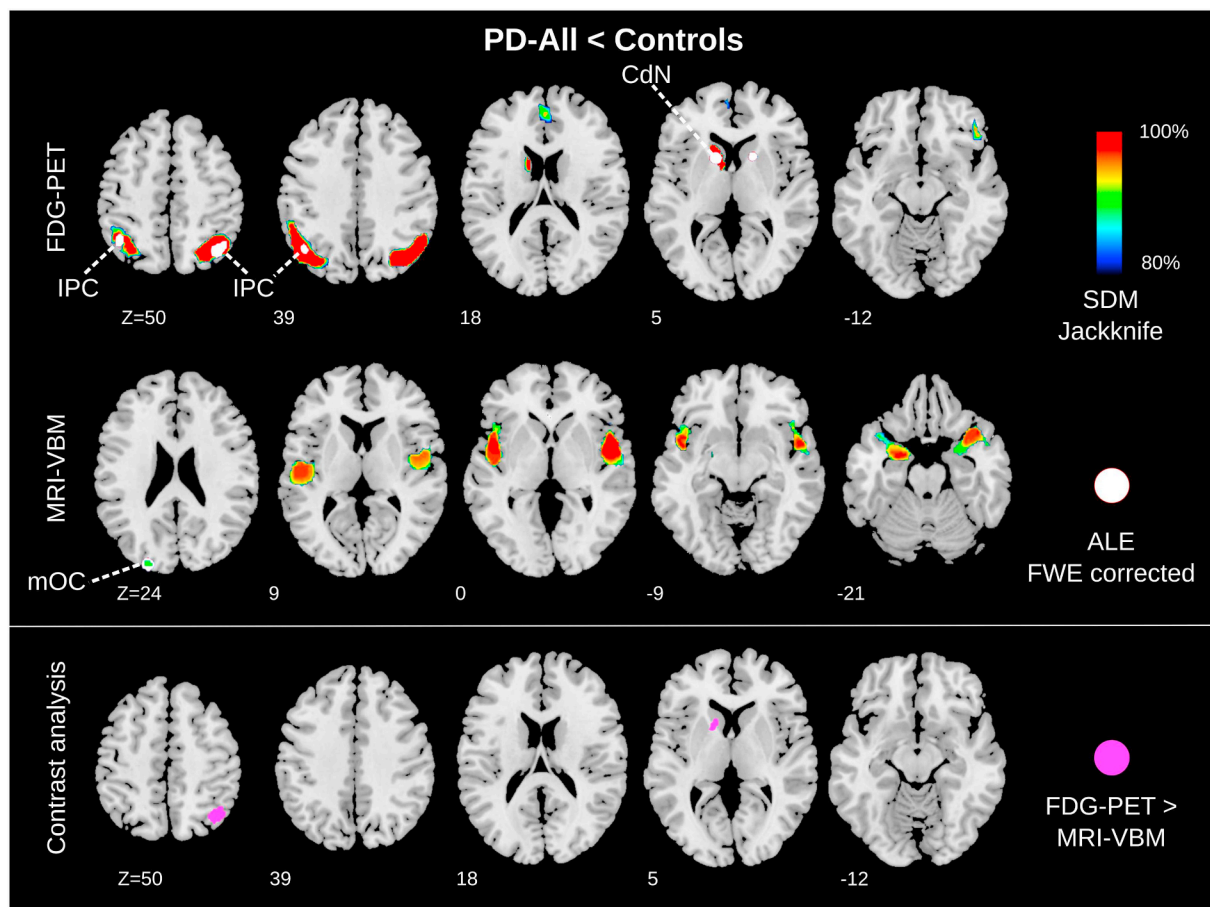

Fig. 2. Hypometabolism and atrophy in Parkinson's disease (PD) patients compared to controls. Upper rows: Meta-analysis of FDG-PET (249 PD/186 controls) and MRI-VBM (1292 PD/1014 controls) studies. The SDM∩ALE conjunction highlights brain regions consistently found in both analyses. Anatomical regions are highlighted only for these consistent results. Bottom row: The contrast analysis shows significant regions for the contrast FDG-PET > MRI-VBM. Images shown in neurological convention in MNI space.
Abbreviations: ALE Anatomical Likelihood Estimation, CdN caudate nucleus, FDG-PET [18F]-fluorodeoxyglucose-positron emission tomography, FWE Family-Wise Error rate, IPC inferior parietal cortex, mOC middle occipital cortex, MRI-VBM voxel-based morphometry analysis of magnetic resonance imaging, PD-All cohort of all PD patients, SDM Seed-based *D* mapping.

3. Results

3.1. Included studies

The PRISMA (Moher et al., 2009) flowchart, describing the selection procedure, is displayed in Fig. 1. The overall meta-analysis included 2323 PD patients and 1767 healthy controls. Out of the total 74 studies, 50 implemented structural MRI (VBM), including 1816 PD patients. Fourteen FDG-PET studies investigated 295 patients and ten whole-brain DTI studies comprised 212 patients. Only studies reporting significant findings are displayed in Table e-1. Notably, negative findings (i.e. no difference comparing patients and controls) were reported in 14 (28% out of all) MRI studies, 3 (21.4%) FDG-PET, and 3 (30%) DTI studies (Table e-2). As for the clinical subgroups, Table 1 displays the number of subjects in each category stratified by imaging modalities.

3.2. Demographic and clinical characteristics

Considering significant studies, Table 1 displays means and standard deviations of descriptive variables for the entire sample, the clinical subgroups, and the imaging modalities. Overall, the mean age of PD patients was 65.6 ± 5.5 years (MRI 66.0 ± 5.8; PET 65.9 ± 4.9; DTI 62.5 ± 4.6) with a good balance between males and females (m/f) 927/728 (MRI 711/561; PET 107/92; DTI 82/56). Disease duration was on average 7.2 ± 4.4 years (MRI 7.1 ± 4.5; PET 8.4 ± 4.6; DTI 5.4 ± 2.6).

Kruskal-Wallis tests showed no significant differences across imaging modalities for age ($\chi^2 = 3.0$), disease duration ($\chi^2 = 1.9$), and severity (UPDRS-III $\chi^2 = 5.9$, MMSE $\chi^2 = 1.2$), guaranteeing a well-matched analysis with balanced variables. For disease severity assessed with the Hoehn & Yahr scale there was a significant difference between the groups ($\chi^2 = 9.0$, df = 2, $p = .011$). The results should be interpreted with care, though, as 46% of the included studies did not report and/or assess Hoehn & Yahr stage, 39% did not report MMSE, and 19% did not report UPDRS-III. Accordingly, studies' comparability in UPDRS-III scores seems to be more valid than the difference in Hoehn & Yahr stages. Note that only two studies (Watanabe et al., 2013; Yarnall et al., 2014) used the MDS-UPDRS scale (Goetz et al., 2008) instead of the UPDRS scale (Fahn, 1987).

3.3. Meta-analysis on the PD-All cohort

Overlapping results of SDM and ALE were deemed significant and are here reported. The PD-All < Controls comparison revealed significant glucose hypometabolism in the entire PD cohort in the bilateral inferior parietal cortex and in the left caudate nucleus, independently of the meta-analytical approach implemented (Fig. 2, top row, and Table 2, e-3, e-4). The conjunction analysis of the PD-All < Controls contrast revealed small focal gray matter atrophy in the middle occipital gyrus (Fig. 2, middle row, and Table 2, e-5, e-6).

3.4. Contrast analyses

The contrast analysis between FDG-PET and MRI-VBM showed only significant findings in the FDG-PET > MRI-VBM contrast. Namely, FDG-PET compared to MRI-VBM revealed brain changes in the left caudate nucleus and right superior parietal cortex/precuneus (Fig. 2, bottom row Table e-10).

3.5. Meta-analysis on subcohorts

The results of the meta-analysis of the subcohorts are displayed in Fig. 3.

PD-Cog: Glucose metabolism was reduced in the bilateral inferior parietal cortex and in the right orbitofrontal cortex with both meta-analytical algorithms in the PD-Cog < Controls comparison, i.e. in PD

patients with cognitive deficits (Fig. 3 and Table e-3, e-4). Conversely, the conjunction analysis of SDM and ALE for the structural MRI meta-analysis showed no overlap. ALE detected atrophy in left hippocampus only, while using SDM atrophy was seen in left insula, putamen, claustrum, and right putamen, as well as in the globus pallidus (Fig. 3, left side, Table e-5, e-6).

PD-Motor: The conjunction analysis on FDG-PET results revealed consistent glucose hypometabolism in the PD-Motor < Controls comparison, i.e. PD patients with solely motor impairment, in the left caudate nucleus, a motor structure. For structural MRI (Fig. 3, right side, and Table e-3, e-4), the ALE meta-analyses did not provide significant results for the PD-Motor cohort.

PD-Inc: Right side of Fig. 3 and Table e-5 and e-6 display findings of higher gray matter density in PD compared to controls (PD-Inc > Controls). An overlap between SDM and ALE was found in basal ganglia, i.e. caudate nucleus, putamen, globus pallidus, and thalamus.

White matter (DTI): DTI studies revealed lower fractional anisotropy in PD compared to controls with consistent results for SDM and ALE in the cingulate bundle close to the orbital and anterior cingulate gyri (Fig. 3, bottom row, and Table e-7, e-8).

White matter (MRI-VBM): The conjunction analysis revealed white matter atrophy in superior longitudinal fasciculus, internal capsule, and extreme/external capsule in the vicinity of the right putamen and globus pallidus in PD compared to controls. White matter atrophy was further found in the superior occipitofrontal fasciculus, corpus callosum, corona radiata, external and internal capsule surrounding the left caudate nucleus (Fig. 3, bottom row, and Table e-5, e-6).

4. Discussion

In summary, our multimodal meta-analysis across whole-brain imaging studies revealed that FDG-PET glucose hypometabolism is more consistently associated with PD as compared to brain atrophy as identified by MRI-VBM. Moreover, the meta-analysis on the subcohorts provides an interesting initial glimpse into specific neural signatures of different PD clinical phenotypes and into white matter changes in PD.

4.1. FDG-PET hypometabolism is more specific than MRI-VBM structural changes in PD

We hypothesize that the reason behind the dissociation between FDG-PET and MRI-VBM results lies in the different PD-related brain changes captured by the two techniques. Indeed, structural MRI analyzed with VBM identifies morphological brain abnormalities (Ashburner and Friston, 2000), while FDG-PET is a proxy of early neuronal injury and synaptic dysfunction. Such functional brain alterations may antedate morphological changes by several years, as in the case of Alzheimer's disease or Huntington's disease (Mosconi, 2013; Tang et al., 2013). Indeed, FDG-PET studies have shown Alzheimer's disease-related brain hypometabolism in cognitively intact subjects at genetic risk (i.e. ε4 homozygous carriers) several years before disease onset (Reiman et al., 1996). Similarly, multimodal imaging studies, combining FDG-PET and structural MRI to investigate presymptomatic genetic Alzheimer's disease, have shown that hypometabolism precedes and exceeds atrophy in the early identification of brain abnormalities (Gordon et al., 2018; Mosconi et al., 2006). In line with that, metabolic changes were shown to be more sensitive to progression of the disease than structural changes in preclinical Huntington's disease mutation carriers (Tang et al., 2013). Thus, in analogy with Alzheimer's disease and Huntington's disease, FDG-PET might be a more accurate biomarker for subtle brain abnormalities in PD. Of note, cohorts in FDG-PET and MRI-VBM studies did not differ regarding age, disease duration, and disease severity, making respective biases unlikely. Although differences in Hoehn & Yahr stage were evident, this comparison was less reliable due to multiple missing data.

Since functional brain changes seem to be more relevant for PD

Table 2
Results for the PD-All cohort.

Cluster #	Volume (mm³)	ALE Value	x	y	z	Region
Local maxima of ALE analyses in FDG-PET						
1	1424	0.022737322	−14	12	4	Left caudate body
2	1416	0.015668042	−42	−56	50	Left inferior parietal lobule
		0.015623625	−44	−62	36	Left middle temporal gyrus
3	1336	0.023226662	38	−64	48	Right precuneus
4	856	0.017095294	16	12	4	Right caudate body
Local maxima of ALE analyses in MRI						
1	976	0.0337	−24	−90	24	Left middle occipital gyrus

Cluster #	Voxels	SDM-Z	x	y	z	Region
Local maxima of SDM analyses in FDG-PET						
1	2217	−4.015	−50	−62	38	Left angular gyrus
2	2070	−3.528	34	−72	38	Right middle occipital gyrus
3	568	−2.894	0	46	20	Left superior medial frontal gyrus
4	466	−3.185	−6	14	4	Left caudate nucleus
5	186	−2.804	46	30	−12	Right inferior frontal gyrus
6	45	−2.590	−44	46	−2	Left middle frontal gyrus
7	43	−2.695	14	12	2	Right anterior thalamic projections
8	28	−2.509	46	26	28	Right inferior frontal gyrus
9	27	−2.506	62	−32	−12	Right middle temporal gyrus
10	26	−2.508	14	−94	16	Right cuneus cortex
11	25	−2.537	60	−50	−6	Right middle temporal gyrus
12	22	−2.574	8	−90	2	Right calcarine fissure
Local maxima of SDM analyses in MRI						
1	1952	−3.304	−24	−2	−18	Left amygdala
2	1804	−3.345	50	2	2	Right rolandic operculum
3	33	−2.746	−24	−90	24	Left superior occipital gyrus

Clusters below an effect-size estimate (SDM) threshold $p < .001$ and an anatomical likelihood estimate (ALE) threshold $p < .05$ FWE are listed. Coordinates are in MNI space.

assessment, also resting-state functional MRI (rs-fMRI) could be employed to investigate the neural signature of PD. Indeed, recent meta-analyses on rs-fMRI studies in PD revealed functional alterations in patients compared to controls in both motor (i.e. supplementary motor areas, left putamen and premotor cortex) and non-motor (i.e. bilateral inferior parietal and supramarginal gyri) networks (Pan et al., 2017; Tahmasian et al., 2017). This result aligns with our FDG-PET findings, pointing out that functional changes both inside and outside the motor network, namely in the inferior parietal cortex, might represent a crucial hallmark of PD that has been neglected so far. Indeed, the inferior parietal cortex is a higher order associative region that plays an important role in various mechanisms ranging from language (e.g. selecting gestures, verbal integration of complex contexts like sentences) to spatial orientation (e.g. processing personal space, localization of objects) as well as motor functions (e.g. tactile reception of complex movements and interaction with objects) (Culham and Kanwisher, 2001). There is even evidence of mirror neurons in the inferior parietal cortex, which encode goals of motor acts (Rizzolatti et al., 2009). Impairment in this region can lead to the well-described effect of spatial hemineglect and further to dysfunction in autobiographical memory, as in the case of Alzheimer's disease, and visual disorientation or mislocalization (Berryhill et al., 2007; Culham and Kanwisher, 2001; Schroeter et al., 2009).

Moreover, we found consistent hypometabolism in the PD-all cohort in the left caudate nucleus, a core structure in the basal ganglia network that, together with the putamen, serves as input structure for nigrostriatal projections (Fallon, 1988). Of note, the conjunction analysis showed a consistent hypometabolism in the left, but not right, caudate nucleus. Different reasons may account for this finding. First, majority of patients with PD present and progress in their parkinsonism unilaterally. In the recent diagnostic criteria by Postuma et al. (2015) bilateral motor symptoms at onset are even considered as a red flag to exclude the diagnosis of PD. Second, SDM additionally identified the right caudate nucleus as compromised by PD, suggesting that our

unilateral finding may have been due to statistical power effects or the differences in algorithms.

Moreover, the result of a consistent caudate hypometabolism in the PD-motor subgroup, but not in the PD-Cog subgroup, is to a certain extent surprising. On the one hand, several previous studies have drawn a link between caudate nuclei function and cognitive deficits – mainly executive functions (Grahn et al., 2008) – in PD with and without dementia (Apostolova et al., 2010; Polito et al., 2012). On the other hand, motor symptoms, particularly rigidity and bradykinesia, are generally associated with dysfunctions in the posterior putamen that shows an earlier and faster decline in dopamine function as compared to the caudate nucleus (Pavese and Brooks, 2009). However, an interesting observation comes from a dual-tracer PET study from Holtbernd et al. (2015) that investigated the relationship between dopaminergic dysfunction and glucose metabolism in a large PD cohort. The study reports significant correlations between dopamine function in the caudate nucleus and the expression of both motor- and cognition-related metabolic patterns in PD, while dopaminergic activity in the putamen was related only to the expression of the motor-related PD pattern. This result supports the role of the posterior putamen in PD motor impairment, while the involvement of the caudate nucleus seems to be implicated in both cognitive and motor symptoms. Of note, many of the studies showing involvement of the putamen in PD by means of FDG-PET applied spatial covariance analysis and reported relative increases in glucose metabolism in the putamen (Eckert et al., 2007). This approach is intrinsically different from the univariate voxel-based statistics implemented by the FDG-PET studies that were object of the present meta-analytical work.

Notably, the subcohort analyses on the FDG-PET data revealed that glucose hypometabolism in cortical associative parietal regions is mainly related to cognitive impairment in PD, while hypometabolism in the caudate nucleus is more strongly associated with the motor phenotype. This might indicate that functional changes outside the basal ganglia are more associated with the presence of cognitive deficits in
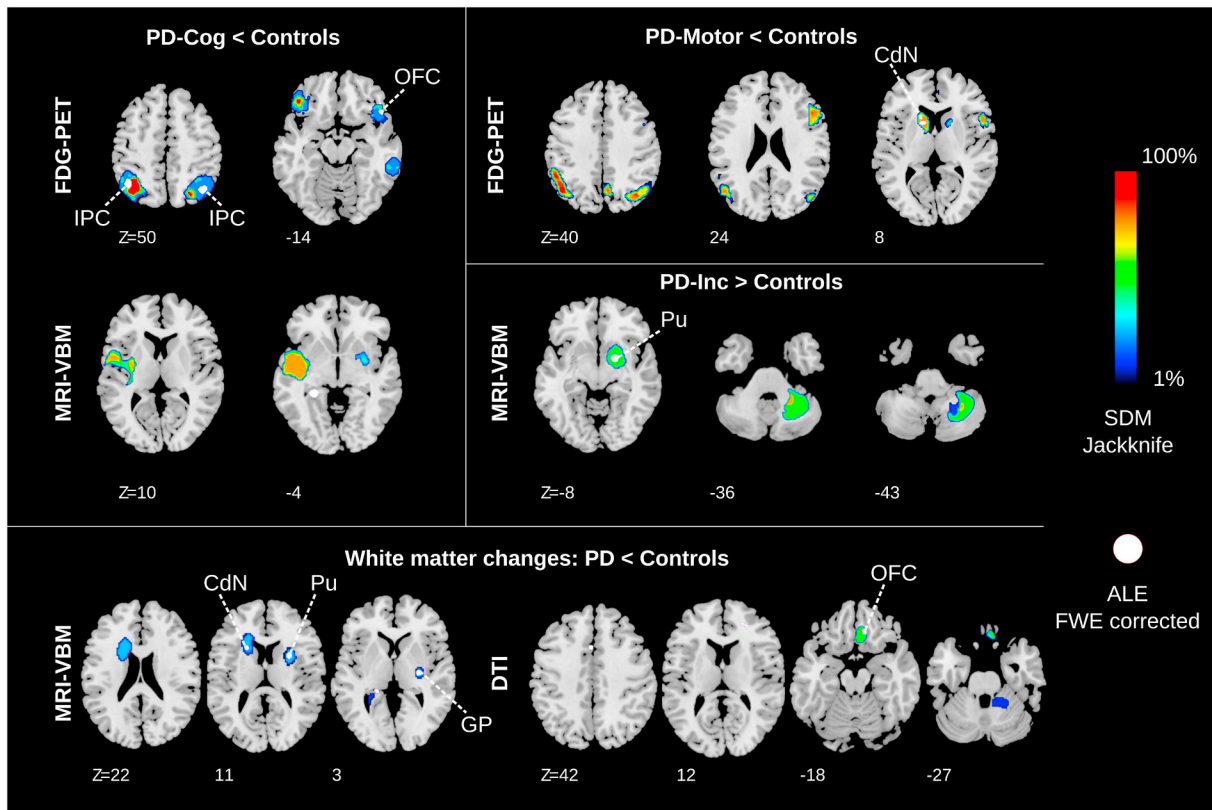
Fig. 3. Hypometabolism and atrophy across Parkinson's disease (PD) clinical subgroups and white matter changes comparing PD to controls. The SDM∩ALE conjunction highlights brain regions consistently found in both analysis algorithms. Anatomical regions are highlighted only for these consistent results. Images shown in neurological convention in the MNI space.

Abbreviations: ALE Anatomical Likelihood Estimation, CdN projections surrounding caudate nucleus, DTI diffusion tensor imaging, FDG-PET [18F]-fluorodeoxyglucose-positron emission tomography, FWE Family-Wise Error rate, GP projections surrounding globus pallidus, IPC inferior parietal cortex, MRI-VBM voxel-based morphometry analysis of magnetic resonance imaging, OFC orbitofrontal cortex, PD-Cog PD with cognitive impairment, PD-Inc gray matter increases in PD, PD-Motor idiopathic PD with only motor symptoms, PU putamen/projections surrounding putamen, SDM Seed-based *D* mapping.

PD, as previously suggested (Huang et al., 2007; Lopes et al., 2017). Hypometabolism in parietal associative areas is also a hallmark of Alzheimer's disease, thus limiting the specificity of our finding as PD biomarker (Schroeter et al., 2009). Also the caudate nucleus, due to its connectivity with prefrontal regions, may play a role in the emergence of cognitive dysfunction in PD beside motor deficits (Brück et al., 2000). Disease specificity of glucose hypometabolism in this brain region for PD is not guaranteed as it has also been reported in behavioral variant frontotemporal dementia and nonfluent/agrammatic variant of primary progressive aphasia (synonymous with progressive non-fluent aphasia) (Bisenius et al., 2016; Schroeter et al., 2014).

Remarkably, five out of the 14 FDG-PET studies reported hypermetabolism in PD as compared to controls, but no significant result was found applying the meta-analytical procedure. Relative metabolic increases in the putamen, globus pallidus, pons and cerebellum have been consistently reported as a crucial feature of the PD-related spatial covariance pattern (Eckert et al., 2007). However, the identification of real FDG-PET hypermetabolism in PD has been questioned, as increased glucose metabolism could be the result of the intensity normalization procedure applied in PET analysis. For example, Borghammer et al. (2009) showed that regional (i.e. mainly subcortical) metabolic increases in PD as compared to controls might artifactually emerge as a consequence of global mean normalization when lower global values characterize the patient group. A comparable finding has been reported for Alzheimer's disease and frontotemporal lobar degeneration (Dukart et al., 2011). However, (Ma et al., 2009) reported that global values in early PD stages are identical to those of healthy controls and that subcortical metabolic increases also correlate with clinical measures. In

our meta-analysis, studies reporting hypermetabolism in PD, especially in subcortical structures, applied global mean normalization, while none of the studies that used either normalization to white matter, cerebellum, pons or absolute FDG-PET measures found increased metabolism. This fact might support the assumption of artefactual increases in metabolism due to normalization to the global mean, although other reasons are still possible. Table e-9 reports different intensity normalization procedures for FDG-PET studies.

Finally, our meta-analysis considered whole-brain FDG-PET studies generally applying univariate statistics to compare patients and controls. A consistent body of literature on multivariate network analysis has also demonstrated the usefulness of FDG-PET (Eidelberg, 2009). Several studies identified the so-called *PD-related covariance pattern (PDRP)* that distinguishes PD patients from healthy controls (Niethammer and Eidelberg, 2012). This metabolic pattern has high accuracy (sensitivity 84%, specificity 97%) in differentiating PD from atypical parkinsonism, is modulated by treatment and is predictive for disease progression (Niethammer and Eidelberg, 2012; Tang et al., 2010). This supports the relevance of functional brain changes as PD biomarkers, which in future might be improved by focusing analyses on the prototypical networks identified in our meta-analyses.

4.2. MRI-VBM changes in PD are heterogeneous and unspecific

In contrast with FDG-PET, we did not find a specific consistent pattern of structural brain changes in PD as detected by whole-brain MRI-VBM analysis. This was also apparent in the contrast analyses where we obtained significant differences only for the FDG-

PET > MRI-VBM contrast. The PD-all < controls comparison revealed only minor atrophy in the middle occipital gyrus. Similarly to our study, also previous meta-analyses investigating structural changes in PD showed only minor and heterogeneous changes (Pan et al., 2012; Shao et al., 2014; Shao et al., 2015; Yu et al., 2015). Furthermore, the high number of MRI-VBM studies reporting null findings for the patients vs. controls comparison indicates that gray matter changes in PD are unspecific and heterogeneous. Additionally, the neuropathological criteria for PD only describe morphological changes in the substantia nigra pars compacta and Lewy pathology as specific pathological signatures of PD even in late phases of the disease (Dickson et al., 2009). Concerning the subcohort analyses, both the meta-analyses in PD with solely motor (PD-Motor) and additional cognitive symptoms (PD-Cog) did not reveal consistent results between the two meta-analytical approaches. This further confirms the inadequacy of atrophy and structural MRI in PD. Notwithstanding, implementing structural MRI could be more useful in the diagnostic workout when guided by a priori hypothesis (e.g. focusing on the substantia nigra) and applying recent technical MRI improvements, such as relaxometry, magnetization transfer, and neuromelanin-sensitive imaging (Lehericy et al., 2012). In addition, more sophisticated machine learning approaches have been proposed for the detection of morphometric PD imaging biomarker, providing high accuracy in differentiating PD patients and controls (Peng et al., 2017).

Surprisingly, we found higher gray matter volume in the right lentiform nucleus and thalamus in PD compared to controls. According to Braak's staging model of disease spreading, the degeneration of the thalamic nuclei is a PD hallmark (Braak et al., 2003). The higher gray matter volume might be a compensatory mechanism to counteract the reduction of inhibitory input to the thalamus (Lin et al., 2013). Indeed, it has been proposed that PD leads to a reduction of the inhibitory input from the globus pallidus and the substantia nigra to the thalamus and a consequent derangement of the thalamic excitatory output to the cortex.

4.3. White matter changes: preliminary evidence

Voxel-wise white matter changes were investigated with both MRI-VBM and DTI. The former revealed widespread white matter changes, while the latter indicated the cingulate bundle near the orbital and anterior cingulate gyri as more affected. These findings are in line with the non-motor symptoms of PD. Orbitofrontal gyri are involved in sniffing and smelling (Sobel et al., 1998). Notably, olfactory dysfunction is one of the earliest features of prodromal PD, preceding disease onset by years to decades (Postuma et al., 2015). The anterior cingulate cortex has been associated with behavioral symptoms in PD (Tekin and Cummings, 2002). However, generalizability of these findings is undermined by the small number of studies in the analysis. As aforementioned, combining the knowledge from histopathological findings and in vivo brain imaging could provide a more accurate PD biomarker. Indeed, DTI studies that focused on the substantia nigra have shown high accuracy in discriminating PD patients from healthy controls (Cochrane and Ebmeier, 2013).

4.4. Limitations of the study

This is, to our knowledge, the largest whole-brain meta-analysis comparing PD patients and controls and the only multimodal study combining MRI, FDG-PET, and DTI. The replicability of our findings is assured by the combination of independent meta-analytic algorithms. Nevertheless, we recognize some limits. First, all included studies lack PD histopathological confirmation, as studies on autopsy-proven cases are extremely rare. Second, methodological and technical differences exist among the included studies, e.g. in field-strength of MR scanners, processing protocols, or data modulation. However, the impact of these differences on our results is limited since the meta-analytical algorithms only take maxima into account and not the cluster size that is more

affected by this heterogeneity. Additionally, our study could not disentangle the influence of pharmacological treatment on PD and the disease process itself, because almost all studies investigated medicated subjects. The aim of our meta-analysis was to identify PD-specific imaging biomarkers to support the diagnosis in the earliest disease stages. However, most of the included studies were performed with patients who have had the disease for several years (mostly in intermediate disease phase), making sub-meta-analyses for early PD unfeasible. We believe that defining biomarkers on subjects in moderate disease stages and applying them at earlier time points, i.e. in *de-novo* patients or even in pre-symptomatic subjects, is a valid approach. This research strategy has been successfully applied in the case of Alzheimer's disease (see for example Bateman et al., 2012; Mosconi et al., 2004; Whitwell et al., 2007). Finally, we remark once again the exploratory nature of the subcohort analysis given the limited number of included studies. Accordingly, future validation of the meta-analysis in independent cohorts is necessary. Specificity and sensitivity of the suggested PD-specific brain regions for differential diagnosis should be validated in large, preferably multicenter, and independent patient cohorts. This approach has already been successfully applied to other neurodegenerative diseases such as Alzheimer's disease and frontotemporal lobar degeneration (Dukart et al., 2013; Dukart et al., 2011). As for the DTI studies, we recognize that the choice of focusing on whole-brain investigations reduced the number of included studies and penalized the results of its diagnostic accuracy. Indeed, as aforementioned, the in vivo tractography of the projections of the substantia nigra provided promising results in classifying patients with PD (Haller et al., 2012).

5. Conclusion

This multimodal and cross-validation meta-analysis aimed at exploring potential imaging biomarkers for PD beyond dopaminergic imaging. The novelty of the meta-analysis is to statistically validate convergence of published results and hence draw solid conclusions with a higher statistical power than single studies. Consistent glucose hypometabolism was found in bilateral inferior parietal cortex and left caudate nucleus combining both meta-analytic methods. Glucose hypometabolism in PD was confirmed in subcohort analyses and related to cognitive deficits (inferior parietal cortex) and motor symptoms (caudate nucleus). Structural MRI showed only small focal gray matter atrophy in the middle occipital gyrus that could not be confirmed in subcohort analyses. DTI revealed fractional anisotropy reduction in the cingulate bundle in the vicinity of the orbital and anterior cingulate gyri in PD. Our meta-analysis suggests that, when applying data-driven whole-brain analysis to neuroimaging data, functional changes as assessed by FDG-PET better characterize PD as compared to structural alterations investigated by MRI-VBM and DTI. Results suggest focusing the search of PD imaging biomarkers on functional rather than structural brain abnormalities. To date neither atrophy nor glucose hypometabolism offer disease-specific imaging biomarkers for PD as the latter regionally overlaps with other neurodegenerative diseases.

Authors' roles

1) Research project: A. Conception: FA, TB, MLS
B. Organization: FA, TB.
C. Execution: FA, TB.
2) Statistical Analysis: A. Design: FA, TB, MLS.
B. Execution: FA, TB.
C. Review and Critique: FA, TB, JN, MLS.
3) Manuscript: A. Writing of the first draft: FA, TB
B. Review and Critique: FA, TB, JN, MLS.

Appendix A. Supplementary data

Table e-1 (All included studies reporting significant findings), Table e-2 (Studies reporting null findings included in the SDM analyses), Table e-3 (FDG-PET maxima ALE), Table e-4 (FDG-PET maxima SDM), Table e-5 (MRI maxima ALE), Table e-6 (MRI maxima SDM), Table e-7 (DTI maxima ALE), Table e-8 (DTI maxima SDM), Table e-9 (Intensity normalization procedures in FDG-PET studies), Table e-10 (Local maxima of contrast analysis), Table e-11 (Differences between ALE and SDM).

References

Albert, M.S., ST, DeKosky, Dickson, D.F., Dubois, B., Feldman, H., Fox, N.C., Gamst, A., Holtzman, D.M., Jagust, W.J., Petersen, R.C., Snyder, P.J., Carrillo, M.C., Thies, B., Phelps, C.H., 2011. The Diagnosis of Mild Cognitive Impairment Due to Alzheimer's Disease: Recommendations from the National Institute on Aging-Alzheimer's Association Workgroups on Diagnostic Guidelines for Alzheimer's Disease.

Apostolova, L.G., Beyer, M., Green, A.E., Hwang, K.S., Morra, J.H., Chou, Y.Y., Avedissian, C., Aarsland, D., Janvin, C.C., Larsen, J.P., 2010. Hippocampal, caudate, and ventricular changes in Parkinson's disease with and without dementia. Mov. Disord. 25, 687–695.

Ashburner, J., Friston, K.J., 2000. Voxel-based morphometry – the methods. NeuroImage 11, 805–821.

Bateman, R.J., Xiong, C., Benzinger, T.L., Fagan, A.M., Goate, A., Fox, N.C., Marcus, D.S., Cairns, N.J., Xie, X., Blazey, T.M., 2012. Clinical and biomarker changes in dominantly inherited Alzheimer's disease. N. Engl. J. Med. 367, 795–804.

Berryhill, M.E., Phuong, L., Picasso, L., Cabeza, R., Olson, I.R., 2007. Parietal lobe and episodic memory: bilateral damage causes impaired free recall of autobiographical memory. J. Neurosci. 27, 14415–14423.

Bisenius, S., Neumann, J., Schroeter, M.L., 2016. Validating new diagnostic imaging criteria for primary progressive aphasia via anatomical likelihood estimation meta-analyses. Eur. J. Neurol. 23, 704–712.

Borghammer, P., Cumming, P., Aanerud, J., Gjedde, A., 2009. Artefactual subcortical hyperperfusion in PET studies normalized to global mean: lessons from Parkinson's disease. NeuroImage 45, 249–257.

Braak, H., Del Tredici, K., Rub, U., de Vos, R.A., Jansen Steur, E.N., Braak, E., 2003. Staging of brain pathology related to sporadic Parkinson's disease. Neurobiol. Aging 24, 197–211.

Brück, A., Portin, R., Lindell, A., Laihinen, A., Bergman, J., Haaparanta, M., Solin, O., Rinne, J.O., 2000. Positron Emission Tomography Shows that Impaired Frontal Lobe Functioning in Parkinson's Disease Is Related to Dopaminergic Hypofunction in the Caudate Nucleus.

Cochrane, C.J., Ebmeier, K.P., 2013. Diffusion tensor imaging in parkinsonian syndromes: a systematic review and meta-analysis. Neurology 80, 857–864.

Culham, J.C., Kanwisher, N.G., 2001. Neuroimaging of cognitive functions in human parietal cortex. Curr. Opin. Neurobiol. 11, 157–163.

Dickson, D.W., Braak, H., Duda, J.E., Duyckaerts, C., Gasser, T., Halliday, G.M., Hardy, J., Leverenz, J.B., Del Tredici, K., Wszolek, Z.K., Litvan, I., 2009. Neuropathological assessment of Parkinson's disease: refining the diagnostic criteria. Lancet Neurol. 8, 1150–1157.

Dubois, B., Feldman, H.H., Jacova, C., Hampel, H., Molinuevo, J.L., Blennow, K., DeKosky, S.T., Gauthier, S., Selkoe, D., Bateman, R., Cappa, S., Crutch, S., Engelborghs, S., Frisoni, G.B., Fox, N.C., Galasko, D., Habert, M.O., Jicha, G.A., Nordberg, A., Pasquier, F., Rabinovici, G., Robert, P., Rowe, C., Salloway, S., Sarazin, M., Epelbaum, S., de Souza, L.C., Vellas, B., Visser, P.J., Schneider, L., Stern, Y., Scheltens, P., Cummings, J.L., 2014. Advancing research diagnostic criteria for Alzheimer's disease: the IWG-2 criteria. Lancet Neurol. 13, 614–629.

Dukart, J., Mueller, K., Horstmann, A., Barthel, H., Moller, H.E., Villringer, A., Sabri, O., Schroeter, M.L., 2011. Combined evaluation of FDG-PET and MRI improves detection and differentiation of dementia. PLoS One 6, e18111.

Dukart, J., Mueller, K., Barthel, H., Villringer, A., Sabri, O., Schroeter, M.L., Alzheimer's Disease Neuroimaging Initiative, 2013. Meta-analysis based SVM classification enables accurate detection of Alzheimer's disease across different clinical centers using FDG-PET and MRI. Psychiatry Res. 212, 230–236.

Eckert, T., Tang, C., Eidelberg, D., 2007. Assessment of the progression of Parkinson's disease: a metabolic network approach. Lancet Neurol. 6, 926–932.

Eickhoff, S.B., Bzdok, D., Laird, A.R., Kurth, F., Fox, P.T., 2012. Activation likelihood estimation meta-analysis revisited. NeuroImage 59, 2349–2361.

Eidelberg, D., 2009. Metabolic brain networks in neurodegenerative disorders: a functional imaging approach. Trends Neurosci. 32, 548–557.

Fahn, S., 1987. Unified Parkinson's disease rating scale. In: Recent Developments in Parkinson's Disease Volume II. Macmillan Healthcare Information, pp. 153.

Fallon, J.H., 1988. Topographic organization of ascending dopaminergic projections. Ann. N. Y. Acad. Sci. 537, 1–9.

Goetz, C.G., Tilley, B.C., Shaftman, S.R., Stebbins, G.T., Fahn, S., Martinez-Martin, P., Poewe, W., Sampaio, C., Stern, M.B., Dodel, R., Dubois, B., Holloway, R., Jankovic, J., Kulisevsky, J., Lang, A.E., Lees, A., Leurgans, S., LeWitt, P.A., Nyenhuis, D., Olanow, C.W., Rascol, O., Schrag, A., Teresi, J.A., van Hilten, J.J., LaPelle, N., Movement Disorder Society UPDRS Revision Task Force, 2008. Movement Disorder Society-sponsored revision of the Unified Parkinson's Disease Rating Scale (MDS-UPDRS): scale presentation and clinimetric testing results. Mov. Disord. 23, 2129–2170.

Gordon, B.A., Blazey, T.M., Su, Y., Hari-Raj, A., Dincer, A., Flores, S., Christensen, J., McDade, E., Wang, G., Xiong, C., Cairns, N.J., Hassenstab, J., Marcus, D.S., Fagan, A.M., Jack Jr., C.R., Hornbeck, R.C., Paumier, K.L., Ances, B.M., Berman, S.B., Brickman, A.M., Cash, D.M., Chhatwal, J.P., Correia, S., Forster, S., Fox, N.C., Graff-Radford, N.R., la Fougere, C., Levin, J., Masters, C.L., Rossor, M.N., Salloway, S., Saykin, A.J., Schofield, P.R., Thompson, P.M., Weiner, M.M., Holtzman, D.M., Raichle, M.E., Morris, J.C., Bateman, R.J., Benzinger, T.L.S., 2018. Spatial patterns of neuroimaging biomarker change in individuals from families with autosomal dominant Alzheimer's disease: a longitudinal study. Lancet Neurol. 17, 241–250.

Gorno-Tempini, M.L., Hillis, A.E., Weintraub, S., Kertesz, A., Mendez, M., Cappa, S.F., Ogar, J.M., Rohrer, J.D., Black, S., Boeve, B.F., Manes, F., Dronkers, N.F., Vandenberghe, R., Rascovsky, K., Patterson, K., Miller, B.L., Knopman, D.S., Hodges, J.R., Mesulam, M.M., Grossman, M., 2011. Classification of primary progressive aphasia and its variants. Neurology 76, 1006–1014.

Grahn, J.A., Parkinson, J.A., Owen, A.M., 2008. The cognitive functions of the caudate nucleus. Prog. Neurobiol. 86, 141–155.

Haller, S., Badoud, S., Nguyen, D., Garibotto, V., Lovblad, K.O., Burkhard, P.R., 2012. Individual detection of patients with Parkinson disease using support vector machine analysis of diffusion tensor imaging data: initial results. AJNR Am. J. Neuroradiol. 33, 2123–2128.

Holtbernd, F., Ma, Y., Peng, S., Schwartz, F., Timmermann, L., Kracht, L., Fink, G.R., Tang, C.C., Eidelberg, D., Eggers, C., 2015. Dopaminergic correlates of metabolic network activity in Parkinson's disease. Hum. Brain Mapp. 36, 3575–3585.

Huang, C., Mattis, P., Tang, C., Perrine, K., Carbon, M., Eidelberg, D., 2007. Metabolic brain networks associated with cognitive function in Parkinson's disease. NeuroImage 34, 714–723.

Hughes, A.J., Ben-Shlomo, Y., Daniel, S.E., Lees, A.J., 1992. What features improve the accuracy of clinical diagnosis in Parkinson's disease: a clinicopathologic study. Neurology 42 (6), 1142.

Kaasinen, V., Vahlberg, T., 2017. Striatal dopamine in Parkinson disease: a meta-analysis of imaging studies. Ann. Neurol. 82, 873–882.

Laird, A., Eickhoff, S., Kurth, F., Fox, P., Uecker, A., Turner, J., Robinson, J., Lancaster, J., Fox, P., 2009. ALE meta-analysis workflows via the BrainMap database: progress towards a probabilistic functional brain atlas. Front. Neuroinform. 3.

Lehericy, S., Sharman, M.A., Dos Santos, C.L., Paquin, R., Gallea, C., 2012. Magnetic resonance imaging of the substantia nigra in Parkinson's disease. Mov. Disord. 27, 822–830.

Lehericy, S., Vaillancourt, D.E., Seppi, K., Monchi, O., Rektorova, I., Antonini, A., McKeown, M.J., Masellis, M., Berg, D., Rowe, J.B., Lewis, S.J.G., Williams-Gray, C.H., Tessitore, A., Siebner, H.R., International Parkinson and Movement Disorder Society (IPMDS)-Neuroimaging Study Group, 2017. The role of high-field magnetic resonance imaging in parkinsonian disorders: pushing the boundaries forward. Mov. Disord. 32, 510–525.

Lin, C.H., Chen, C.M., Lu, M.K., Tsai, C.H., Chiou, J.C., Liao, J.R., Duann, J.R., 2013. VBM reveals Brain volume differences between Parkinson's disease and essential tremor patients. Front. Hum. Neurosci. 7, 247.

Lopes, R., Delmaire, C., Defebvre, L., Moonen, A.J., Duits, A.A., Hofman, P., Leentjens, A.F., Dujardin, K., 2017. Cognitive phenotypes in Parkinson's disease differ in terms of brain-network organization and connectivity. Hum. Brain Mapp. 38, 1604–1621.

Lotankar, S., Prabhavalkar, K.S., Bhatt, L.K., 2017. Biomarkers for Parkinson's disease: recent advancement. Neurosci. Bull. 33, 585–597.

Ma, Y., Tang, C., Moeller, J.R., Eidelberg, D., 2009. Abnormal regional brain function in Parkinson's disease: truth or fiction? NeuroImage 45, 260–266.

Moher, D., Liberati, A., Tetzlaff, J., Altman, D.G., PRISMA-Group, 2009. Preferred reporting items for systematic reviews and meta-analyses: the PRISMA statement. BMJ 339, b2535.

Mosconi, L., 2013. Glucose metabolism in normal aging and Alzheimer's disease: methodological and physiological considerations for PET studies. Clin. Transl. Imag. 1.

Mosconi, L., Perani, D., Sorbi, S., Herholz, K., Nacmias, B., Holthoff, V., Salmon, E., Baron, J.-C., De Cristofaro, M., Padovani, A., 2004. MCI conversion to dementia and the APOE genotype a prediction study with FDG-PET. Neurology 63, 2332–2340.

Mosconi, L., Sorbi, S., de Leon, M.J., Li, Y., Nacmias, B., Myoung, P.S., Tsui, W., Ginestroni, A., Bessi, V., Fayyazz, M., Caffarra, P., Pupi, A., 2006. Hypometabolism exceeds atrophy in presymptomatic early-onset familial Alzheimer's disease. J. Nucl. Med. 47, 1778–1786.

Niethammer, M., Eidelberg, D., 2012. Metabolic brain networks in translational neurology: concepts and applications. Ann. Neurol. 72, 635–647.

Pan, P.L., Song, W., Yang, J., Huang, R., Chen, K., Gong, Q.Y., Zhong, J.G., Shi, H.C., Shang, H.F., 2012. Gray matter atrophy in behavioral variant frontotemporal dementia: a meta-analysis of voxel-based morphometry studies. Dement. Geriatr. Cogn. Disord. 33, 141–148.

Pan, P., Zhang, Y., Liu, Y., Zhang, H., Guan, D., Xu, Y., 2017. Abnormalities of regional brain function in Parkinson's disease: a meta-analysis of resting state functional magnetic resonance imaging studies. Sci. Rep. 7, 40469.

Pavese, N., Brooks, D.J., 2009. Imaging neurodegeneration in Parkinson's disease. Biochim. Biophys. Acta (BBA) - Mol. Basis Dis. 1792, 722–729.

Peng, B., Wang, S., Zhou, Z., Liu, Y., Tong, B., Zhang, T., Dai, Y., 2017. A multilevel-ROI-features-based machine learning method for detection of morphometric biomarkers in Parkinson's disease. Neurosci. Lett. 651, 88–94.

Poewe, W., Seppi, K., Tanner, C.M., Halliday, G.M., Brundin, P., Volkmann, J., Schrag, A.E., Lang, A.E., 2017. Parkinson disease. Nat. Rev. Dis. Primers 3, 17013.

Polito, C., Berti, V., Ramat, S., Vanzi, E., De Cristofaro, M.T., Pellicanò, G., Mungai, F., Marini, P., Formiconi, A.R., Sorbi, S., 2012. Interaction of caudate dopamine depletion and brain metabolic changes with cognitive dysfunction in early Parkinson's disease. Neurobiol. Aging 33, 206.e229–206.e239.

Postuma, R.B., Berg, D., 2016. Advances in markers of prodromal Parkinson disease. Nat. Rev. Neurol. 12, 622–634.

Postuma, R.B., Berg, D., Stern, M., Poewe, W., Olanow, C.W., Oertel, W., Obeso, J., Marek, K., Litvan, I., Lang, A.E., Halliday, G., Goetz, C.G., Gasser, T., Dubois, B., Chan, P., Bloem, B.R., Adler, C.H., Deuschl, G., 2015. MDS clinical diagnostic criteria for Parkinson's disease. Mov. Disord. 30, 1591–1601.

Radua, J., Mataix-Cols, D., 2009. Voxel-wise meta-analysis of grey matter changes in obsessive-compulsive disorder. Br. J. Psychiatry 195, 393–402.

Radua, J., Mataix-Cols, D., 2012. Meta-analytic methods for neuroimaging data explained. Biol. Mood Anxiety Disord 2, 6.

Radua, J., Rubia, K., Canales-Rodríguez, E.J., Pomarol-Clotet, E., Fusar-Poli, P., Mataix-Cols, D., 2014. Anisotropic kernels for coordinate-based meta-analyses of neuroimaging studies. Front. Psychol. 5, 13.

Rascovsky, K., Hodges, J.R., Knopman, D., Mendez, M.F., Kramer, J.H., Neuhaus, J., van Swieten, J.C., Seelaar, H., Dopper, E.G., Onyike, C.U., Hillis, A.E., Josephs, K.A., Boeve, B.F., Kertesz, A., Seeley, W.W., Rankin, K.P., Johnson, J.K., Gorno-Tempini, M.L., Rosen, H., Prioleau-Latham, C.E., Lee, A., Kipps, C.M., Lillo, P., Piguet, O., Rohrer, J.D., Rossor, M.N., Warren, J.D., Fox, N.C., Galasko, D., Salmon, D.P., Black, S.E., Mesulam, M., Weintraub, S., Dickerson, B.C., Diehl-Schmid, J., Pasquier, F., Deramecourt, V., Lebert, F., Pijnenburg, Y., Chow, T.W., Manes, F., Grafman, J., Cappa, S.F., Freedman, M., Grossman, M., Miller, B.L., 2011. Sensitivity of revised diagnostic criteria for the behavioural variant of frontotemporal dementia. Brain 134, 2456–2477.

Reiman, E.M., Caselli, R.J., Yun, L.S., Chen, K., Bandy, D., Minoshima, S., Thibodeau, S.N., Osborne, D., 1996. Preclinical evidence of Alzheimer's disease in persons homozygous for the epsilon 4 allele for apolipoprotein E. N. Engl. J. Med. 334, 752–758.

Rizzolatti, G., Fabbri-Destro, M., Cattaneo, L., 2009. Mirror neurons and their clinical relevance. Nat. Clin. Pract. Neurol. 5, 24.

Schapira, A.H.V., Chaudhuri, K.R., Jenner, P., 2017. Non-motor features of Parkinson disease. Nat. Rev. Neurosci. 18, 435–450.

Schroeter, M.L., Stein, T., Maslowski, N., Neumann, J., 2009. Neural correlates of Alzheimer's disease and mild cognitive impairment: a systematic and quantitative meta-analysis involving 1351 patients. NeuroImage 47, 1196–1206.

Schroeter, M.L., Laird, A.R., Chwiesko, C., Deuschl, C., Schneider, E., Bzdok, D., Eickhoff, S.B., Neumann, J., 2014. Conceptualizing neuropsychiatric diseases with multimodal data-driven meta-analyses - the case of behavioral variant frontotemporal dementia. Cortex 57, 22–37.

Shao, N., Yang, J., Li, J., Shang, H.F., 2014. Voxelwise meta-analysis of gray matter anomalies in progressive supranuclear palsy and Parkinson's disease using anatomic likelihood estimation. Front. Hum. Neurosci. 8, 63.

Shao, N., Yang, J., Shang, H., 2015. Voxelwise meta-analysis of gray matter anomalies in Parkinson variant of multiple system atrophy and Parkinson's disease using anatomic likelihood estimation. Neurosci. Lett. 587, 79–86.

Sobel, N., Prabhakaran, V., Desmond, J.E., Glover, G.H., Goode, R.L., Sullivan, E.V., Gabrieli, J.D., 1998. Sniffing and smelling: separate subsystems in the human olfactory cortex. Nature 392, 282–286.

Tahmasian, M., Eickhoff, S.B., Giehl, K., Schwartz, F., Herz, D.M., Drzezga, A., van Eimeren, T., Laird, A.R., Fox, P.T., Khazaie, H., Zarei, M., Eggers, C., Eickhoff, C.R., 2017. Resting-state functional reorganization in Parkinson's disease: an activation likelihood estimation meta-analysis. Cortex 92, 119–138.

Tang, C.C., Poston, K., Eckert, T., Feigin, A., Frucht, S., Gudesblatt, M., Dhawan, V., Lesser, M., Vonsattel, J.-P., Fahn, S., Eidelberg, D., 2010. Differential diagnosis of parkinsonism: a metabolic imaging study using pattern analysis. Lancet Neurol. 9 (2), 149–158.

Tang, C.C., Feigin, A., Ma, Y., Habeck, C., Paulsen, J.S., Leenders, K.L., Teune, L.K., van Oostrom, J.C.H., Guttman, M., Dhawan, V., Eidelberg, D., 2013. Metabolic network as a progression biomarker of premanifest Huntington's disease. J. Clin. Invest. 123, 4076–4088.

Tekin, S., Cummings, J.L., 2002. Frontal–subcortical neuronal circuits and clinical neuropsychiatry: an update. J. Psychosom. Res. 53, 647–654.

Titova, N., Padmakumar, C., Lewis, S.J.G., Chaudhuri, K.R., 2017. Parkinson's: a syndrome rather than a disease? J. Neural Transm. (Vienna) 124, 907–914.

Tuite, P., 2017. Brain magnetic resonance imaging (MRI) as a potential biomarker for Parkinson's disease (PD). Brain Sci. 7.

Watanabe, H., Senda, J., Kato, S., Ito, M., Atsuta, N., Hara, K., Tsuboi, T., Katsuno, M., Nakamura, T., Hirayama, M., Adachi, H., Naganawa, S., Sobue, G., 2013. Cortical and subcortical brain atrophy in Parkinson's disease with visual hallucination. Mov. Disord. 28, 1732–1736.

Whitwell, J.L., Przybelski, S.A., Weigand, S.D., Knopman, D.S., Boeve, B.F., Petersen, R.C., Jack Jr., C.R., 2007. 3D maps from multiple MRI illustrate changing atrophy patterns as subjects progress from mild cognitive impairment to Alzheimer's disease. Brain 130, 1777–1786.

Yarnall, A.J., Breen, D.P., Duncan, G.W., Khoo, T.K., Coleman, S.Y., Firbank, M.J., Nombela, C., Winder-Rhodes, S., Evans, J.R., Rowe, J.B., Mollenhauer, B., Kruse, N., Hudson, G., Chinnery, P.F., O'Brien, J.T., Robbins, T.W., Wesnes, K., Brooks, D.J., Barker, R.A., Burn, D.J., ICICLE-PD Study Group, 2014. Characterizing mild cognitive impairment in incident Parkinson disease: the ICICLE-PD study. Neurology 82, 308–316.

Yu, F., Barron, D.S., Tantiwongkosi, B., Fox, P., 2015. Patterns of gray matter atrophy in atypical parkinsonism syndromes: a VBM meta-analysis. Brain Behav. 5, e00329.